J Physiol Sci (2013) 63:113–123
DOI 10.1007/s12576-012-0243-6

ORIGINAL PAPER

A new calpain inhibitor protects left ventricular dysfunction induced by mild ischemia-reperfusion in in situ rat hearts

D. Takeshita · M. Tanaka · S. Mitsuyama · Y. Yoshikawa · G. -X. Zhang · K. Obata · H. Ito · S. Taniguchi · Miyako Takaki

Received: 18 September 2012 / Accepted: 25 November 2012 / Published online: 16 December 2012

Abstract We have previously indicated that a new soluble calpain inhibitor, SNJ-1945 (SNJ), attenuates cardiac dysfunction after cardioplegia arrest-reperfusion by inhibiting the proteolysis of α-fodrin in in vitro study. Nevertheless, the in vivo study design is indispensable to explore realistic therapeutic approaches for clinical use. The aim of the present in situ study was to investigate whether SNJ attenuated left ventricular (LV) dysfunction (stunning) after mild ischemic-reperfusion (mI-R) in rat hearts. SNJ (60 μmol/l, 5 ml i.p.) was injected 30 min before gradual and partial coronary occlusion at proximal left anterior descending artery. To investigate LV function, we obtained curvilinear end-systolic pressure–volume relationship by increasing afterload 60 min after reperfusion. In the mI-R group, specific LV functional indices at midrange LV volume (mLVV), end-systolic pressure (ESP_{mLVV}), and pressure–volume area (PVA_{mLVV}: a total mechanical energy per beat, linearly related to oxygen consumption) significantly decreased, but SNJ reversed these decreases to time control level. Furthermore, SNJ prevented the α-fodrin degradation and attenuated degradation of Ca^{2+} handling proteins after mI-R. Our results indicate that improvements in LV function following mI-R injury are associated with inhibition of the proteolysis of α-fodrin in in situ rat hearts. In conclusion, SNJ should be a promising tool to protect the heart from the stunning.

Keywords Mild ischemic-reperfusion injury · Cardioprotection · α-Fodrin · SNJ-1945

Abbreviations

BW	Body weight
Ea	Arterial effective elastance
E–C	Excitation–contraction
EDV	End-diastolic volume
EF	Ejection fraction
ESP	End-systolic pressure
ESP_{ESV}	End-systolic pressure at end-systolic volume
ESP_{mLVV}	End-systolic pressure at mLVV
ESPVR	End-systolic pressure–volume relationship
ESV	End-systolic volume
HR	Heart rate
I-R	Ischemic-reperfusion
LTCC	L-type Ca^{2+} channel
LV	Left ventricular
LVP	Left ventricular pressure
LVV	Left ventricular volume
LVW	LV weight
mI-R	Mild ischemic-reperfusion
mLVV	Midrange LVV
NCX	Na^{+}–Ca^{2+} exchanger
P–V	Pressure–volume

D. Takeshita and M. Tanaka contributed equally to this work.

D. Takeshita · M. Tanaka · S. Mitsuyama · G.-X. Zhang · K. Obata · H. Ito · M. Takaki (✉)
Department of Physiology II, Nara Medical University School of Medicine, 840 Shijo-cho, Kashihara, Nara 634-8521, Japan
e-mail: mtakaki@naramed-u.ac.jp

M. Tanaka
Faculty of Health Care Science, Himeji Dokkyo University, Himeji, Japan

Y. Yoshikawa · S. Taniguchi
Department of Thoracic and Cardiovascular Surgery, Nara Medical University, Nara, Japan

G.-X. Zhang
Department of Physiology, Medical College of Soochow University, Dushu Lake Campus, Suzhou Industrial Park, Suzhou 215123, People's Republic of China

PVA_{mLVV}	Systolic pressure–volume area at mLVV
SERCA2a	Sarcoplasmic reticulum Ca^{2+} ATPase
SV	Stroke volume

Introduction

It is well known that one of underlying mechanisms for ischemic-reperfusion (I-R) injury is Ca^{2+} overload resulting from increased Ca^{2+} influx mediated via reverse-mode Na^{+}–Ca^{2+} exchanger (NCX) [1–4]. We have previously reported that reperfusion injury after KCl cardioplegic cardiac arrest leads to Ca^{2+} overload and the resultant left ventricular (LV) dysfunction similar to I-R injury [5]. The mechanisms of Ca^{2+} overload in this model are likely accumulation of intracellular Na^{+} and subsequent activation of reverse-mode NCX activity [6]. However, previous studies in our laboratory suggest that proteolysis of the cytoskeletal protein α-fodrin by calpains may also play a role in LV dysfunction [5, 7, 8].

Calpain inhibition was found to prevent the proteolysis of α-fodrin due to reperfusion injury after global ischemia [8] and after KCl cardioplegic cardiac arrest [9]. It has been proposed that α-fodrin maintains the integrity of the plasma membranes as a constituent of the membrane skeleton [10, 11]. Therefore, it seems likely that the degradation of α-fodrin in membrane fractions would alter the properties of ion channels [12]. Indeed, the possibility that disruption of cytoskeletal proteins inactivates L-type Ca^{2+} channels has been reported [13].

Recently, we have reported that a novel calpain inhibitor, {(1S)-1[(((1S)-1-benzyl-3-cyclopropyl-amino-2,3-dioxopropyl) amino) carbonyl]-3-methylbutyl} carbamic acid 5-methoxy-3-oxapentyl ester (SNJ-1945; SNJ) attenuates left ventricular (LV) dysfunction induced by reperfusion-injury after cardioplegic cardiac arrest, by inhibiting the proteolysis of α-fodrin, without any effects on protein levels of sarcoplasmic reticulum Ca^{2+} ATPase (SERCA2a) and L-type Ca^{2+} channel (LTCC) [9]. This novel calpain inhibitor (SNJ) has been shown to have good aqueous solubility, good plasma exposure, and good tissue penetration in rats and monkeys [14, 15]. Intraperitoneal administration of SNJ (160 mg/kg) for 14 days produced no obvious toxicity or abnormalities in rats [14]. Furthermore, it has been reported that SNJ was effective against cerebral ischemia-induced damage [16], but there have been no reports on its efficacy against cardiac I-R injury in in situ hearts. Only our recent study has reported that SNJ was effective against reperfusion injury after cardioplegic cardiac arrest, though in in vitro hearts [9].

Accordingly, the in vivo study design is indispensable to explore realistic therapeutic approaches for clinical use, since in vivo cardiac hemodynamics is regulated by the autonomic nervous system and endocrine gland. These regulations are lacking in in vitro hearts. The aim of the present study was to investigate the cardioprotective effects of SNJ against mild I-R (mI-R)-induced injury after gradual and partial coronary occlusion at the proximal left anterior descending artery in rat in situ hearts using analysis of LV mechanical work.

Methods

The investigation conformed with the *Guide for the Care and Use of Laboratory Animals* published by the US National Institutes of Health (NIH Publication No. 85-23, revised 1996), and reviewed and approved by the animal care and use committee of Nara Medical University.

Surgical preparation

The trachea was intubated, and the rat was ventilated with room air under pentobarbital (50 mg/kg, i.p.) anesthesia. Body temperature was maintained normal using the warming plate. The chest was opened, and a conductance catheter (1.5 Fr) [17] was introduced into the LV through an apical stab to obtain reliable LV volume (LVV) signal. A 1.5-Fr pressure catheter was also inserted through the apex into the LV to obtain reliable LV pressure (LVP) signal. Anesthetic level was sustained with pentobarbital intravenous infusion at 0.5 mg kg^{-1} h^{-1} throughout the experiment.

Mild ischemic-reperfusion heart preparation

Coronary gradual and partial occlusion was performed in 10 s by ligation of proximal left anterior descending artery and attached 1-mm-diameter soft tube using a bulldog clamp at the knot of suture (Fig. 1a) under monitoring LV pressure–volume (P–V) loop. During this occlusion, the P–V loop moderately shifted rightward and each stroke volume gradually decreased accompanied with increases in heart rate, but end-systolic pressure (ESP) hardly changed (Fig. 1b). The rats did not cause lethal arrhythmia because of adequate perfusion pressure. The total mean survival rate of the protocol was 80.0 ± 7.1 %; 76.9 % in mI-R and 88.2 % in SNJ + mI-R group in the present mI-R injury model. No differences in the occurrence of arrhythmia in the SNJ + mI-R group were observed compared with that in the mI-R group. This preparation is a stunned heart model [18, 19] and appropriate for our LV functional analysis because no myocardial infarctions were observed

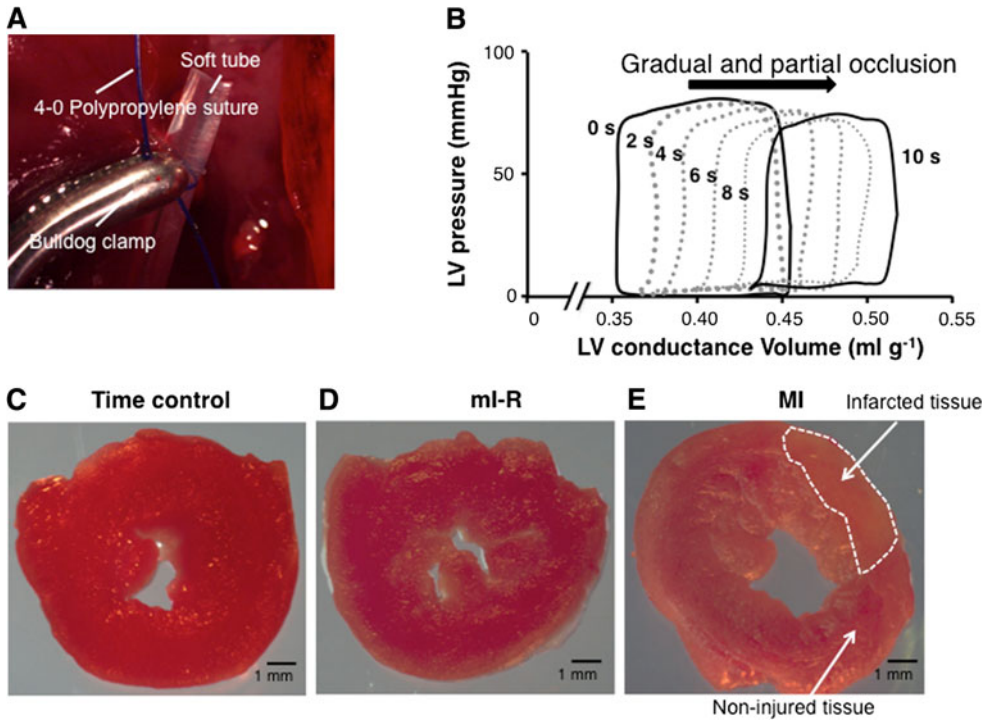

Fig. 1 Mild ischemic-reperfusion (mI-R) heart preparation. **a** Coronary gradual and partial occlusion was performed in 10 s by ligation of proximal left anterior descending artery and attached 1-mm-diameter soft tube (as buffer) using a bulldog clamp at the knot of 4-0 polypropylene suture under monitoring LV pressure–volume (P–V) loop. **b** Typical left ventricular (LV) pressure–volume loops during gradual and partial coronary occlusion to make mild ischemic-reperfusion heart preparations. **c** A typical macrograph of the preparation of time control. **d** A typical LV macrograph of the mI-R preparation obtained 20 min after mI-R. No myocardial infarction was observed. **e** A typical macrograph of the preparation of acute myocardial infarction (MI) obtained 20 min after severe I-R. The infarct tissue was indicated by the *white dotted boundary*. It appeared white even by naked eyes. The non-injured tissue was indicated by an arrow outside the infarct tissue

20 min after reperfusion (Fig. 1d) as previously reported [19], although the mild ischemia period persisted for 30 min in the present protocol.

Measurements of LV stroke volume and pressure volume area (PVA)

Forty-one male Wistar rats (7–12 weeks) were used in the present experiments. The experimental protocol is shown in Fig. 2. LV functions were analyzed in 4 randomly divided groups, i.e., time control, SNJ, mI-R, and SNJ + mI-R. The sample number of SNJ + mI-R was about three times higher than the other groups because it was the most important group to evaluate the effect of SNJ on mI-R.

LV pressure–volume measurements at "Functional analysis" in Fig. 2 were performed 60 min after coronary reperfusion. The detailed methods using conductance and pressure catheters have been described in previous reports [20–23]; LV stroke volume (SV) [=LV end-diastolic volume (EDV) − LV end-systolic volume (ESV)], end-systolic pressure at ESV (ESP_{ESV}) and Ea (arterial effective elastance; ESP_{ESV} SV^{-1}) calculated from steady-state P–V loops were evaluated (Fig. 3a). At midrange LVV (mLVV), end-systolic pressure (ESP_{mLVV}) and systolic pressure–volume area (PVA_{mLVV}, an appropriate index for evaluating cardiac total mechanical energy per beat) calculated from end-systolic pressure–volume relationship (ESPVR) curve, were also evaluated (Fig. 3b).

The LV end-systolic P–V data on the upper left shoulder of multiple P–V loops during increasing afterload by aortic gradual occlusion were plotted and fitted by the method of least squares using the following equation: $LVP = A\{1 - \exp[-B(LVV - V_0)]\}$, where A and B are fitted parameters and V_0 is systolic unstressed volume [20, 23–25]. Aortic gradual occlusion was performed to tighten a string occluder placed loosely around the ascending aorta until EDV increased slightly as previously reported [20, 21].

The PVA as a function of LVV was obtained by integrating the above exponential function from the extrapolated V_0 along the volume axis: $PVA = A(LVV - V_0) - A\{1 - \exp[-B\ (LVV - V_0)]\}/B$ [20, 23–25]. PVA is linearly related to myocardial oxygen consumption per beat [22]. Therefore, PVA_{mLVV} is a better cardiac functional index in terms of cardiac mechanoenergetics. In the present study, we calculated mLVV, which was the value of

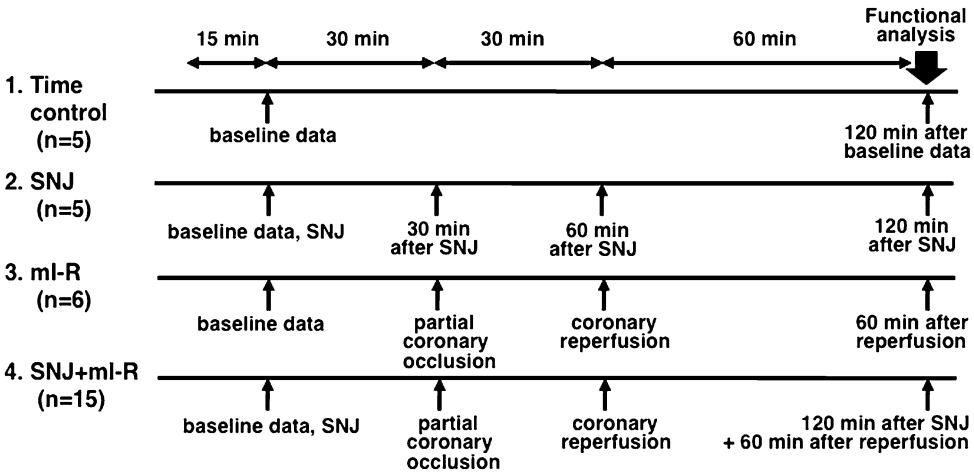

Fig. 2 Experimental protocols of the four groups. *1* Time control group ($n = 5$); *2* SNJ group ($n = 5$); *3* mI-R group ($n = 6$); *4* SNJ + mI-R group ($n = 15$)

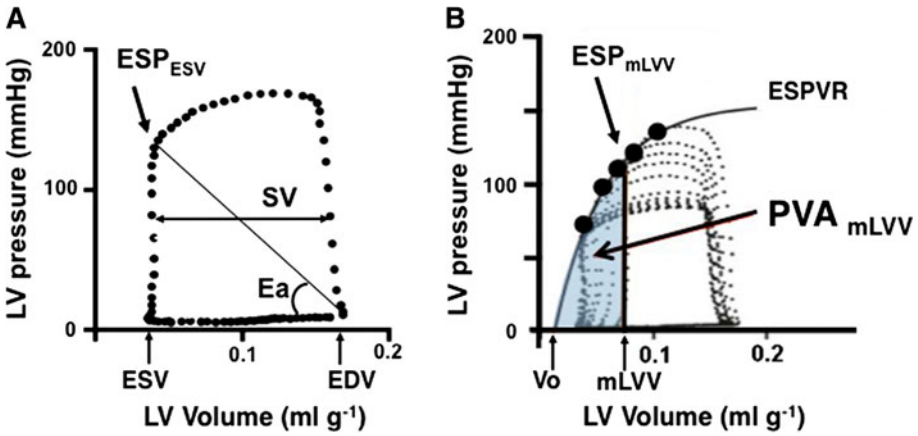

Fig. 3 Evaluation of left ventricular (*LV*) function by end-systolic pressure–volume relation (*ESPVR*) using pressure–volume (P–V) measurements. Enveloping curve of end-systolic pressure at end-systolic volume (ESP_{ESV}) data of several P–V loops during aortic gradual occlusion (gradually increasing afterload) corresponds to ESPVR. *SV* stroke volume, *ESV* end-systolic volume, *EDV* end-diastolic volume, *Ea* effective arterial elastance. *mLVV* midrange LV volume, V_0 LV volume intercept, ESP_{mLVV} end-systolic pressure at mLVV, PVA_{mLVV} systolic pressure–volume area at mLVV

[V_0 + (maximum ESV − minimum ESV) on the ESPVR × 1/2] from all P–V loops in each group [20, 24, 25].

Drugs

A synthetic, water-soluble calpain inhibitor, SNJ-1945, (SNJ: provided from Senju Pharmaceutical, Kobe, Japan) was dissolved in Lactate Ringer solution at 60 μmol/l. Other lipophilic calpain inhibitors, such as MDL28170, calpain inhibitor-3 [26], and calpain inhibitor-1 [8] had been previously dissolved in DMSO, which has antioxidant properties. In the present study, we did not use DMSO to dissolve SNJ and thus our study did not include a vehicle control group. We administered SNJ solution at a dose of 0.387 mg/kg on average (60 μmol/l, 5 ml, i.p.); 60 μmol/l is the limit of its solubility [9]. SNJ has a β_1 receptor stimulating action [27], but in the present study this action was not detected (Tables 2, 3).

Polyacrylamide gel electrophoresis and immunoblottings of 150- and 145-kD fragments of α-fodrin (250-kD), L-type Ca^{2+} channel (LTCC) and sarcoplasmic reticulum Ca^{2+} ATPase (SERCA2a)

Membrane proteins were isolated from the LV wall of each frozen heart stored at −80 °C after the mechanoenergetic studies. The frozen hearts (0.1 g) were homogenized in 1 ml of the STE buffer containing 0.32 mol/l sucrose, 10 mmol/l Tris–HCl, pH 7.4, 1 mmol/l EGTA, 5 mmol/l NaN_3, 10 mmol/l β-mercaptoethanol, 20 mmol/l leupeptin, 0.15 mmol/l pepstatin A, 0.2 mmol/l phenylmethanesulfonyl fluoride, and 50 mmol/l NaF with a Polytron homogenizer (NS-310E; Micotec) and centrifuged at 1,000*g* for 10 min. The supernatants were centrifuged at 100,000*g* for 60 min at 4 °C. The 100,000*g* pellets were cellular membrane fractions. Membrane proteins (50 μg/lane) were subjected to SDS-poly-acrylamide gel electrophoresis,

Table 1 Comparison of cardiac weights among time control, mI-R, SNJ + mI-R, and SNJ groups

	Time control ($n = 5$)	mI-R ($n = 6$)	SNJ + mI-R ($n = 15$)	SNJ ($n = 5$)
BW (g)	436 ± 30.5	319 ± 47.2*	353 ± 60.1*	388 ± 68.7
LVW (g)	0.729 ± 0.062	0.666 ± 0.078	0.676 ± 0.064	0.711 ± 0.174
RVW (g)	0.185 ± 0.021	0.164 ± 0.015	0.166 ± 0.031	0.152 ± 0.053
HW BW^{-1}	2.10 ± 0.068	2.63 ± 0.303*	2.43 ± 0.347	2.20 ± 0.172
LVW BW^{-1}	1.67 ± 0.096	2.11 ± 0.248*	1.95 ± 0.276	1.82 ± 0.138
RVW BW^{-1}	0.426 ± 0.051	0.523 ± 0.082	0.481 ± 0.109	0.383 ± 0.063

Values are mean ± SD. The sample number of SNJ + mI-R was about three times higher than the other groups because this was the most important group to evaluate the effect of SNJ on mI-R

BW body weight, *LVW* left ventricle weight, *RVW* right ventricle weight, *HW* heart weight, HW BW^{-1} the ratio of HW to BW, *LVW* BW^{-1} the ratio of LVW to BW, *RVW* BW^{-1} the ratio of RVW to BW

* $P < 0.05$ versus time control

followed by immunoblotting of 150- and 145-kD fragments of α-fodrin (240-kD)[8, 28, 29], LTCC, and SERCA2a [9]. The membranes were blocked (4 % Block Ace; Dainippon Pharmaceutical, Osaka, Japan) and then incubated with 2,000-fold diluted primary antibody against anti-α-fodrin (1:2,000 dilution, Biohit; Genex), anti-LTCC antibody (1:300 dilution; Alomone Labs, Israel) and anti-SERCA2a antibody (1:1,000 dilution; Affinity Bio Reagents). The antigens were detected by the luminescence method (ECL Western blotting detection kit, Amersham) with peroxidase-linked anti-mouse IgG (1:2,000 dilution) or peroxidase-linked anti-rabbit IgG (1:2,000). The amounts of membrane proteins were determined to obtain the linear response of ECL-immunoblot. After immunoblotting, the film was scanned with a scanner, and the intensity of the bands was calculated by NIH image analysis. The intensity ratio of the 145- and 150-kD bands versus the 240-kD band (α-fodrin) was expressed in an arbitrary unit and compared with that in the time control (average = 1.0).

Statistics

Comparison of paired and unpaired individual values was performed by paired and unpaired *t* test, respectively. Multiple comparisons were performed by one-way analysis of variance (ANOVA) with post hoc Bonferroni's test or Tukey HSD test. A value of $P < 0.05$ was considered statistically significant. All data are expressed as the mean ± SD.

Results

All cardiac weights data comparing among different 4 groups are shown in Table 1. The smaller BWs in the mI-R (7–11 weeks) and SNJ + mI-R (7–11 weeks) groups were due to younger age than that in the time control (10–12 weeks). All mean pre- and post-data comparing among the different 4 groups are shown in Tables 2 and 3. There were no significant differences in any of the hemodynamic indices of ESV, EDV, Ea, and ESP_{ESV} except for post-ESP_{ESV} in mI-R among the time control, mI-R, SNJ + mI-R, and SNJ groups (Table 2).

Effects of SNJ on LV functions

In SNJ group, each mean SV, ESP_{ESV}, Ea, ESP_{mLVV}, and PVA_{mLVV} was not significantly different from each baseline data for 120 min (Tables 2, 3), indicating no β_1 receptor stimulating action was detected under the present experimental conditions.

Effects of SNJ on LV mechanoenergetics after mI-R

A representative set of P–V loops and ESPVRs during aortic occlusion in each group is shown in Fig. 4. In mI-R group, ESPVR markedly shifted downward 60 min after mI-R (Fig. 4b). In contrast, the P–V loops and ESPVR in SNJ + mI-R (Fig. 4c) 30 min before and 60 min after mI-R were similar to those in the time control (Fig. 4a).

Mean fitting parameters, *A* and *B* of ESPVR, in each group are shown in Table 3. In the mI-R group, the post-fitting parameter *A* significantly ($P < 0.05$) decreased compared with the pre-one. This was consistent with a marked downward-shift of ESPVR after mI-R (Fig. 4b). A representative set of PVA–LVV relationship curves calculated using *A* and *B* in each group is shown in Fig. 5. Post-mI-R PVA is decreased at any LVV in the mI-R group, although the larger the LVV, the larger the decrease in PVA that is observed (Fig. 5b).

The mean absolute values of ESP_{mLVV}, PVA_{mLVV} and ESP_{ESV} in each group are also shown in Tables 2 and 3. Post-mI-R mean values of ESP_{mLVV} and PVA_{mLVV} in the mI-R group were significantly ($P < 0.05$) smaller than

Table 2 Hemodynamics in time control, mI-R, SNJ + mI-R, and SNJ groups

	Time control ($n = 5$)	mI-R ($n = 6$)	SNJ + mI-R ($n = 15$)	SNJ ($n = 5$)
ESV (ml)				
Pre	0.062 ± 0.019	0.053 ± 0.024	0.070 ± 0.022	0.078 ± 0.012
Post	0.083 ± 0.042	0.117 ± 0.042	0.116 ± 0.037	0.086 ± 0.017
EDV (ml)				
Pre	0.161 ± 0.040	0.158 ± 0.039	0.165 ± 0.027	0.170 ± 0.025
Post	0.177 ± 0.059	0.209 ± 0.052	0.206 ± 0.041	0.179 ± 0.033
SV (ml)				
Pre	0.098 ± 0.022	0.105 ± 0.019	0.095 ± 0.019	0.092 ± 0.019
Post	0.094 ± 0.021	0.091 ± 0.026	0.090 ± 0.016	0.094 ± 0.016
ESV (ml g^{-1})				
Pre	0.085 ± 0.021	0.081 ± 0.038	0.104 ± 0.036	0.116 ± 0.037
Post	0.113 ± 0.054	0.180 ± 0.071	0.172 ± 0.057	0.125 ± 0.034
EDV (ml g^{-1})				
Pre	0.219 ± 0.042	0.238 ± 0.055	0.245 ± 0.039	0.253 ± 0.071
Post	0.241 ± 0.072	0.318 ± 0.089	0.306 ± 0.061	0.261 ± 0.069
SV (ml g^{-1})				
Pre	0.134 ± 0.023	0.157 ± 0.022	0.140 ± 0.023	0.136 ± 0.039
Post	0.128 ± 0.025	0.138 ± 0.039	0.134 ± 0.024	0.136 ± 0.035
ESP_{ESV} (mmHg)				
Pre	89.7 ± 10.3	90.4 ± 11.3	86.9 ± 9.5	86.5 ± 6.2
Post	88.5 ± 6.4	71.4 ± 10.9*	85.3 ± 12.1	86.9 ± 4.2
Ea (mmHg ml^{-1} g^{-1})				
Pre	681 ± 116	584 ± 105	642 ± 161	686 ± 237
Post	712 ± 149	551 ± 176	651 ± 132	669 ± 159
HR (beats min^{-1})				
Pre	330 ± 21	354 ± 29	369 ± 33	360 ± 30
Post	316 ± 31	342 ± 29	336 ± 38	348 ± 39

To compare volume data among different size of hearts, normalization by LVW is dispensable. Values are mean ± SD. The sample number of SNJ + mI-R was about three times higher than the other groups because this was the most important group to evaluate the effect of SNJ on mI-R

Pre baseline data, *Post* 120 min after baseline data, *mI-R* mild ischemic-reperfusion, *ESV* (*ml*) absolute end-systolic volume, *EDV* (*ml*) absolute end-diastolic volume, *SV* (*ml*) absolute stroke volume, *ESV EDV and SV* (*ml* g^{-1}) each volume normalized by LVW, ESP_{ESV} end-systolic pressure, *Ea* effective arterial elastance (=ESP_{ESV} SV^{-1}), *HR* heart rate

* $P < 0.05$ versus Pre

those in the time control group whereas those in the SNJ + mI-R group were significantly ($P < 0.05$) larger than those in the mI-R group. Post-mI-R mean values of ESP_{mLVV}, PVA_{mLVV}, and ESP_{ESV} in the mI-R group were significantly ($P < 0.05$) smaller than the pre-mI-R mean values whereas those in the SNJ + mI-R group were not significantly different from the pre-mI-R mean values.

The mean % of baseline data in ESP_{mLVV}, PVA_{mLVV}, and ESP_{ESV} significantly ($P < 0.05$) decreased compared to the time control group (=100 %) and that in SV moderately decreased but not significantly in the mI-R group (Fig. 6b). In the SNJ + mI-R group, the mean % of baseline data in ESP_{mLVV}, PVA_{mLVV}, and ESP_{ESV} significantly ($P < 0.05$) increased from those in the mI-R group to time control level (Fig. 6a, c, d).

Immunoblotting of 150- and 145-kD fragments of α-fodrin (240-kD)

Figure 7 shows immunoblottings of 240-kD α-fodrin and 145- and 150-kD α-fodrin proteolytic fragments in the time control, mI-R, and SNJ + mI-R groups. The mean amounts of the 145- and 150-kD fragments in the mI-R group were significantly ($P < 0.05$) larger than those in the time control group. The mean amounts of the 145- and 150-kD fragments in the SNJ + mI-R group were significantly ($P < 0.05$) smaller than those in the mI-R group. α-fodrin mean degradation 120 min after SNJ did not increase (1.16 ± 0.34 fold; $n = 5$) compared with the time control group ($n = 3$). The results indicated that α-fodrin degradation after mI-R was completely prevented by SNJ treatment.

Table 3 Variables of left ventricular mechanics in time control, mI-R, SNJ + mI-R, and SNJ groups

ESPVR	Time control ($n = 5$)	mI-R ($n = 6$)	SNJ + mI-R ($n = 15$)	SNJ ($n = 5$)
A (mmHg)				
Pre	151 ± 25.7	153 ± 22.5	144 ± 25.9	130 ± 4.3
Post	126 ± 24.4	101 ± 23.6$^{\$}$	135 ± 33.7	131 ± 11.4
B (ml^{-1})				
Pre	36.4 ± 14.5	21.9 ± 8.5	22.7 ± 13.5	21.9 ± 6.8
Post	53.2 ± 17.7	28.4 ± 16.8*	24.5 ± 13.3*	26.3 ± 6.9*
V_0 (ml g^{-1})	0.058 ± 0.012	0.041 ± 0.037	0.066 ± 0.042	0.077 ± 0.036
mLVV (ml g^{-1})	0.137 ± 0.012	0.141 ± 0.037	0.167 ± 0.042	0.178 ± 0.036
ESP_{mLVV} (mmHg)				
Pre	123.3 ± 9.6	120.1 ± 11.6	115.5 ± 16.4	112.5 ± 14.6
Post	116.2 ± 12.6	85.8 ± 13.7*$^{\$}$	112.1 ± 20.9$^{\#}$	117.4 ± 8.6$^{\#}$
PVA_{mLVV} (mmHg ml beat^{-1} g^{-1})				
Pre	7.81 ± 2.50	8.48 ± 1.47	7.88 ± 1.88	7.73 ± 1.45
Post	7.46 ± 0.87	5.06 ± 1.06*$^{\$}$	7.43 ± 1.61$^{\#}$	7.56 ± 0.47$^{\#}$

End-systolic pressure–volume relationship (ESPVR) curve was obtained by the formula $LVP = A\{1 - \exp[-B(LVV - V_0)]\}$, where A and B are fitted parameters and V_0 is LV volume intercept (=systolic unstressed volume) (11, 15, 17, 25), mLVV is midrange LV volume, ESP_{mLVV} is end-systolic pressure at mLVV. Systolic pressure–volume area (PVA) was obtained by the formula $PVA = A(LVV - V_0) - A\{1 - \exp[-B(LVV - V_0)]\}/B$ (11, 15, 17, 25), where PVA_{mLVV} is PVA at mLVV. Values are mean ± SD. The sample number of SNJ + mI-R was about three times higher than the other groups because this was the most important group to evaluate the effect of SNJ on mI-R

Pre baseline data, *Post* 120 min after baseline data

* $P < 0.05$ versus time control

$^{\#}$ $P < 0.05$ versus mI-R

$^{\$}$ $P < 0.05$ versus Pre

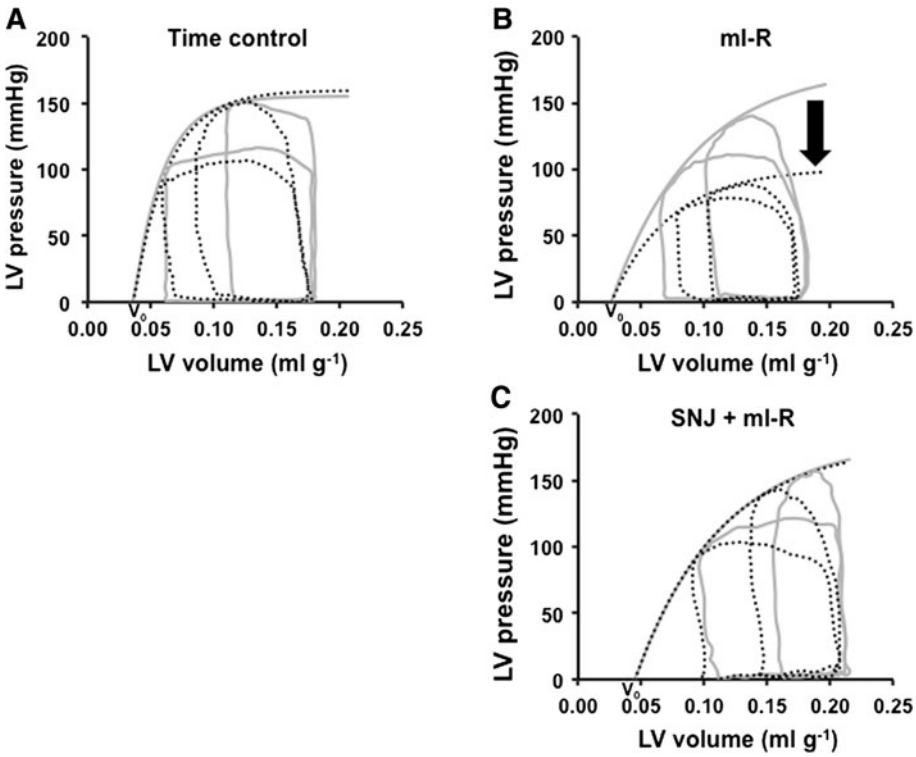

Fig. 4 A representative set of P–V loops and ESPVRs during aortic occlusion in each group. Each onset and offset P–V loop and ESPVRs at baseline and 120 min after baseline are indicated by *gray solid* and *black dotted lines* in the time control group (**a**), respectively. Each onset and offset P–V loop and ESPVRs 30 min before and 60 min after mI-R are indicated by *gray solid* and *black dotted lines* in the mI-R (**b**) and SNJ + mI-R groups (**c**), respectively. *Solid arrow* in **b** indicates downward shift of ESPVR. V_0 LV volume intercept

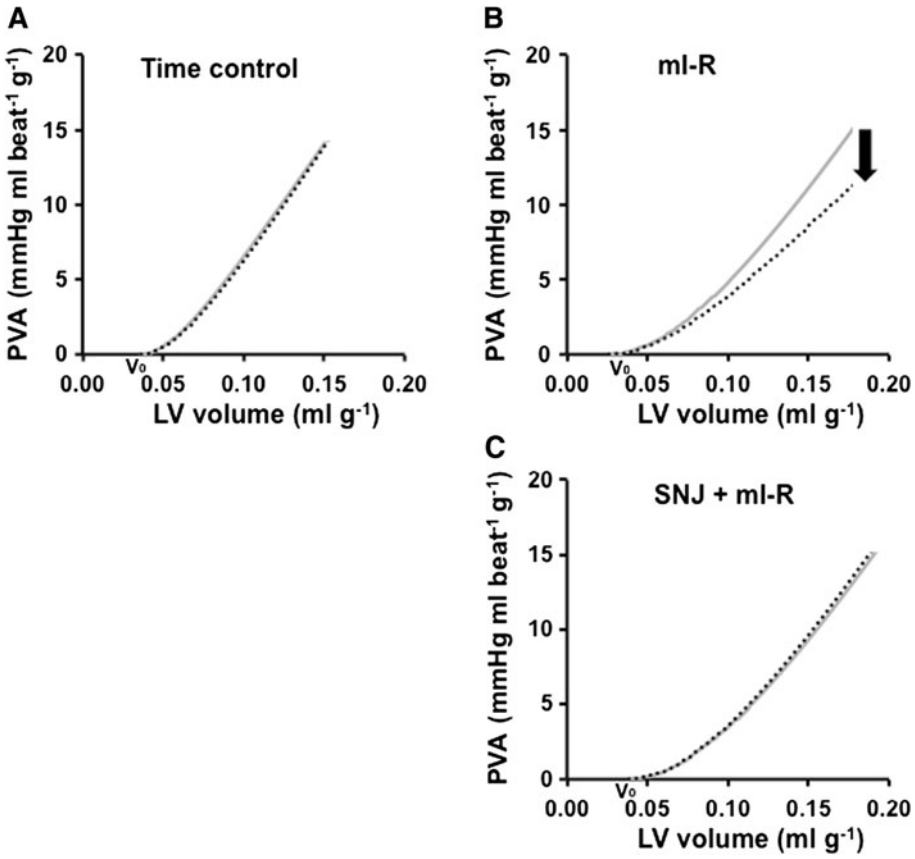

Fig. 5 PVA–LVV relationship curves in the time control (**a**), mI-R (**b**) and SNJ + mI-R groups (**c**), respectively. PVA–LVV relationship curves 30 min before and 60 min after mI-R are indicated by *gray solid* and *black dotted lines*, respectively. *Solid arrow* in **b** indicates downward shift of PVA–LVV relation curve. V_0 LV volume intercept

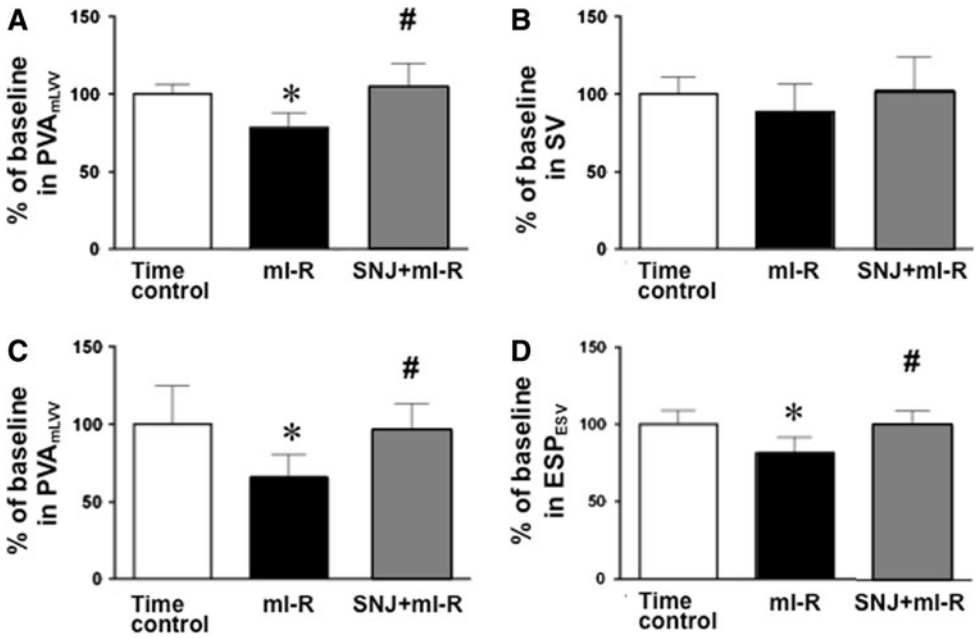

Fig. 6 Mean percent of baseline data in ESP_{mLVV} (**a**), SV (**b**), PVA_{mLVV} (**c**). and ESP_{ESV} (**d**) 60 min after mI-R in each group. Data show the mean with SD. $^{*}P < 0.05$ versus time control, $^{\#}P < 0.05$ versus mI-R

Figure 8a shows immunoblottings of LTCC in the time control, mI-R, and SNJ + mI-R groups. The mean amount of LTCC protein in mI-R was significantly ($P < 0.05$) smaller than that in the time control group. The mean amounts of LTCC protein in the SNJ + mI-R group were not significantly different from those in the time control and mI-R groups. The results indicated that moderate prevention of LTCC degradation after mI-R was attained by SNJ treatment.

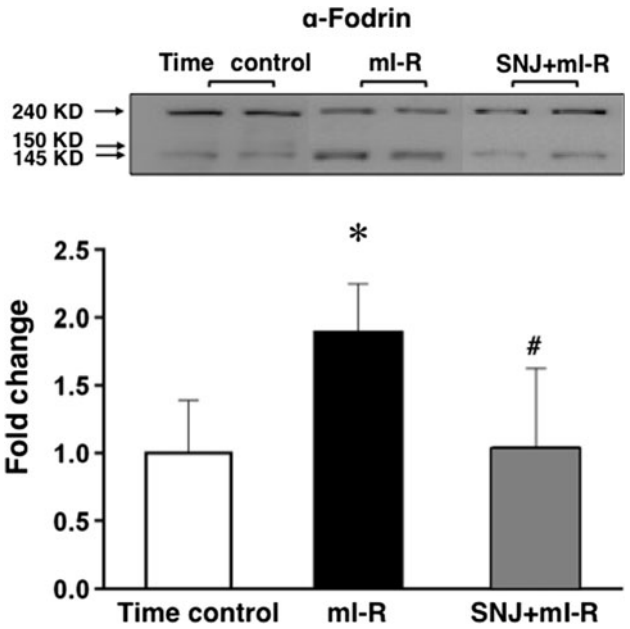

Fig. 7 Ratio of 150- and 145-kD proteolytic fragments by calpain to 240-kD intact α-fodrin in the time control, mI-R, and SNJ + mI-R groups. *Upper panel* each representative band in the time control, mI-R, and SNJ + mI-R groups. All bands were obtained from the same SDS–polyacrylamide gel. *Lower panel* mean fold change of 150- and 145-kD fragments to 240-kD α-fodrin compared to mean value (=1.0) in the time control ($n = 9$) group among the mI-R ($n = 9$) and SNJ + mI-R ($n = 5$) groups. Data show the mean with SD. $^{*}P < 0.05$ versus time control, $^{\#}P < 0.05$ versus mI-R. Immunoblotting of 150- and 145-kD fragments of α-fodrin (240-kD)

Figure 8b shows immunoblottings of SERCA2a in the time control, mI-R, and SNJ + mI-R groups. The mean amount of SERCA2a protein in the mI-R group was significantly ($P < 0.05$) smaller than that in the time control group. The mean amount of SERCA2a protein in the SNJ + mI-R group increased but not significantly ($P > 0.05$) and remained significantly ($P < 0.05$) smaller than that in the time control group, indicating partial prevention of SERCA2a degradation after mI-R was attained by SNJ treatment.

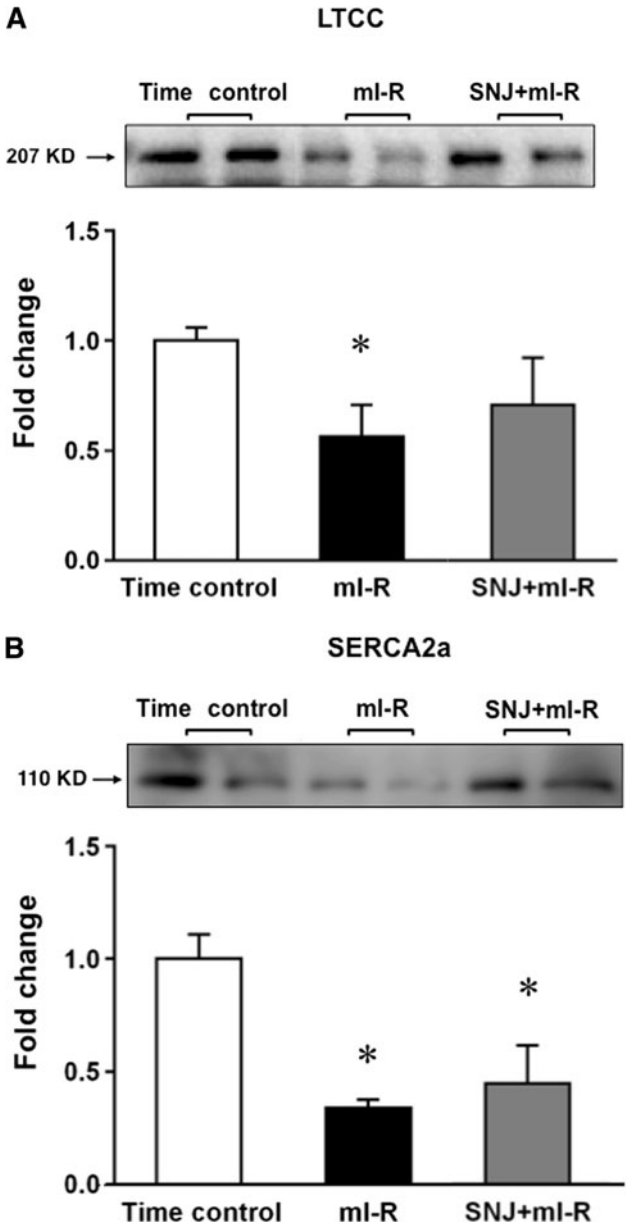

Fig. 8 Comparison of LTCC protein levels (**a**) and SERCA2a (**b**) among the time control, mI-R, and SNJ + mI-R groups. *Upper panels* each representative band in the time control, mI-R, and SNJ + mI-R groups. All bands of LTCC (**a**) and SERCA2a (**b**) were obtained from the same SDS–polyacrylamide gels, respectively. *Lower panels* mean fold changes of LTCC (**a**) and SERCA2a (**b**) compared to the mean value (=1.0) in the time control ($n = 6$) group among the mI-R ($n = 6$) and SNJ + mI-R ($n = 6$) groups. Data show the mean with SD. $^{*}P < 0.05$ versus time control

Discussion

We have previously demonstrated that, in in vitro rat hearts, the lipophilic calpain inhibitor, calpain inhibitor-1, attenuates α-fodrin proteolysis and cardiac dysfunction due to I-R injury [8] and acute Ca^{2+} overload [7]. Recently, we have also demonstrated that a new water-soluble calpain inhibitor, SNJ, exerts similar cardioprotective actions in in vitro rat hearts after KCl (30 mEq) cardioplegia arrest-reperfusion [9]. In the present study, we found that, in in situ rat hearts, pretreatment of SNJ also completely prevented cardiac dysfunction and α-fodrin degradation induced by mI-R.

We have previously reported that proteolysis of a cytoskeleton protein, α-fodrin, is found without proteolysis of ankyrin, connexin 43, and troponin I in high Ca^{2+}-infusion-induced Ca^{2+} overloaded contractile failing hearts associated with the impairment of the total

Ca^{2+} handling in the excitation–contraction (E–C) coupling [7]. It seems likely that α-fodrin is the most sensitive membrane protein to Ca^{2+} overload. To investigate the cardiac protective effect of SNJ mediated via calpain inhibition, we focused on proteolysis of α-fodrin in the present mI-R injury model, because there is a close correlation between the membrane α-fodrin proteolysis and the impairment of the total Ca^{2+} handling [7–9].

In addition, recent studies have revealed that calpain activation induced by I-R injury causes degradation of Ca^{2+}-handling proteins such as LTCC [30] and SERCA2a [26, 30]. Thus, we also examined the degradation of Ca^{2+}-handling proteins such as LTCC and SERCA2a in the present mI-R injury model.

It has been proposed that fodrin maintains the integrity of the plasma membranes as a constituent of the membrane skeleton [10]. Therefore, it seems likely that the degradation of fodrin in membrane fractions would alter the properties of ion channels [12]. From the possibility that disruption of cytoskeletal proteins inactivates LTCC [13, 31], we speculate that the linkage of the LTCC to the membrane fodrin tethers the channel in place, which somehow modulates the basal activity of the channel, and a loss of the linkage may impair its regulation. Therefore, the calpain inhibitor may have protected against LV dysfunction by preserving the structural integrity of the LTCC in the cell membrane [13, 31], as in in vitro rat hearts after cardioplegia arrest-reperfusion [9].

Although the degradation of LTCC and SERCA2a was not identified in reperfusion injury after cardioplegia cardiac arrest in in vitro rat hearts [9], in the present mild I-R injury in in situ rat hearts, the degradation of LTCC and SERCA2a was identified. SNJ attenuated the degradation of LTCC and SERCA2a, though not completely. Therefore, SNJ attenuated cardiac dysfunction, possibly and partially by preventing the dysfunction of Ca^{2+} handling proteins, such as LTCC and possibly SERCA2a. Although the protein level of SERCA2a remained low, large amounts of SERCA2a protein are originally expressed in the rat myocardium, and thus this level may be sufficient if some functional compensation such as activation of phosphorylation of phospholamban occurs mediated via the autonomic nervous system and/or hormonal control system.

We have reported a marked β_1 action of SNJ in the blood-perfused excised rat hearts [27]. However, in the present in situ heart study, no marked β_1 action of SNJ was observed (see Tables 2, 3). The differences between in vitro and in situ studies might have been caused by the different application methods of SNJ. In in vitro hearts, the direct infusion of SNJ into the coronary artery was performed, whereas in in situ hearts, the indirect intraperitoneal injection of SNJ was performed.

In conclusion, a new water-soluble (thus more beneficial for clinical use) calpain inhibitor, SNJ, should be a promising tool for pharmacotherapy to exert cardioprotective actions in clinical setting. Present in situ mild I-R injury model hearts correspond to stunned myocardium around the necrotic focus in acute myocardial infarction in clinical setting. Upon direct percutaneous transluminal coronary angioplasty (PTCA) for acute myocardial infarction, the stunned myocardium generates arrhythmia and myocardial contractile dysfunction. Pretreatment with SNJ upon PTCA would prevent in vivo heart from generating arrhythmia and myocardial dysfunction.

Limitation of the study

The measurement of the expression levels of other Ca^{2+} handling proteins, such as Na^+–Ca^{2+}-exchanger, phospholamban and ryanodine receptor would be expected for better understanding of the function of Ca^{2+} handling in E–C coupling in the future work.

Acknowledgments This work was supported in part by Grants-in-Aid No. 22790216 for Scientific Research from the Ministry of Education, Culture, Sports, Science and Technology of Japan. We also thank Senju Pharmaceutical Co. Ltd., Kobe, for providing us with SNJ-1945.

Conflict of interest None.

References

1. Hagihara H, Yoshikawa Y, Ohga Y, Takenaka C, Murata K, Taniguchi S, Takaki M (2005) Na^+/Ca^{2+} exchange inhibition protects the rat heart from ischemic-reperfusion injury by blocking energy-wasting processes. Am J Physiol Heart Circ Physiol 288:H1699–H1707
2. Karmazyn M, Gan XT, Humphreys RA, Yoshida H, Kusumoto K (1999) The myocardial Na^+/H^+ exchange structure, regulation, and its role in heart disease. Circ Res 85:777–786
3. Schäfer C, Ladilov Y, Inserte J, Schäfer M, Haffner S, Garcia-Dorado D, Piper HM (2001) Role of the reverse mode of the Na^+/Ca^{2+} exchanger in reoxygenation-induced cardiomyocyte injury. Cardiovasc Res 51:241–250
4. Tani M, Neely JR (1989) Role of intracellular Na^+ in Ca^{2+} overload and depressed recovery of ventricular function of reperfused ischemic rat hearts. Possible involvement of H^+–Na^+ and Na^+–Ca^{2+} exchange. Circ Res 65:1045–1056
5. Kobayashi S, Yoshikawa Y, Sakata S, Takenaka C, Hagihara H, Ohga Y, Abe T, Taniguchi S, Takaki M (2004) Left ventricular mechanoenergetics after hyperpolarized cardioplegic arrest by nicorandil and after depolarized cardioplegic arrest by KCl. Am J Physiol Heart Circ Physiol 287:H1072–H1080
6. Opie LH (1998) Myocardial reperfusion, chap. 19. In: The heart. Physiology, from cell to circulation. Lippincott-Raven, Philadelphia, pp 563–588
7. Tsuji T, Ohga Y, Yoshikawa Y, Sakata S, Abe T, Tabayashi N, Kobayashi S, Kitamura S, Taniguchi S, Suga H, Takaki M (2001) Rat cardiac contractile dysfunction induced by Ca^{2+} overload:

possible link to the proteolysis of fodrin. Am J Physiol Heart Circ Physiol 281:H1286–H1294
8. Yoshikawa Y, Hagihara H, Ohga Y, Nakajima-Takenaka C, Murata K, Taniguchi S, Takaki M (2005) Calpain inhibitor-1 protects the rat heart from ischemic-reperfusion injury: analysis by mechanical work and energetics. Am J Physiol Heart Circ Physiol 288:H1690–H1698
9. Yoshikawa Y, Zhang G-X, Obata K, Ohga Y, Matsuyoshi H, Taniguchi S, Takaki M (2010) Cardioprotective effects of a novel calpain inhibitor, SNJ-1945 for reperfusion injury after cardioplegic cardiac arrest. Am J Physiol Heart Circ Physiol 298:H643–H651
10. Bennett V (1990) Spectrin-based membrane skeleton: a multipotential adaptor between plasma membrane and cytoplasm. Physiol Rev 70:1029–1065
11. Lazarides E, Nelson WJ (1983) Erythrocyte and brain forms of spectrin in cerebellum: distinct membrane-cytoskeletal domains in neurons. Science 220:1295–1296
12. Yoshida K, Inui M, Harada K, Saido TC, Sorimachi Y, Ishihara T, Kawashima S, Sobue K (1995) Reperfusion of rat heart after brief ischemia induces proteolysis of calspectin (nonerythroid spectrin or fodrin) by calpain. Circ Res 77:603–610
13. Galli A, DeFelice LJ (1994) Inactivation of L-type Ca channels in embryonic chick ventricle cells: dependence on the cytoskeletal agents colchicine and taxol. Biophys J 67:2296–2304
14. Oka T, Walkup RD, Tamada Y, Nakajima E, Tochigi A, Shearer TR, Azuma M (2006) Amelioration of retinal degeneration and proteolysis in acute ocular hypertensive rats by calpain inhibitor ((1S)-1((((1S)-1-benzyl-3-cyclopropylamino-2,3-di-oxo-propyl) amino) carbonyl)-3-methylbutyl) carbamic acid 5-methoxy-3-oxapentyl ester. Neuroscience 141:2139–2145
15. Shirasaki Y, Yamaguchi M, Miyashita H (2006) Retinal penetration of calpain inhibitors in rats after oral administration. J Ocul Pharmacol 22:417–424
16. Koumura A, Nonaka Y, Hyakkoku K, Oka T, Shimazawa M, Hozumi I, Inuzuka T, Hara H (2008) A novel calpain inhibitor, ((1S)-1((((1S)-1-benzyl-3-cyclopropyl-amino-2,3-di-oxopropyl) amino) carbonyl)-3-methylbutyl) carbamic acid 5-methoxy-3-oxapentyl ester, protects neuronal cells from cerebral ischemia-induced damage in mice. Neuroscience 157:309–318
17. Ito H, Takaki M, Yamaguchi H, Tachibana H, Suga H (1996) Left ventricular volumetric conductance catheter for rats. Am J Physiol 270:H1509–H1514
18. Braunwald E, Kloner RA (1982) The stunned myocardium: prolonged, postischemic ventricular dysfunction. Circulation 66:1146–1149
19. Hamilton KL, Powers SK, Sugiura T, Kim S, Lennon S, Tumer N, Mehta JL (2001) Short-term exercise training can improve myocardial tolerance to I/R without elevation in heat shock proteins. Am J Physiol Heart Circ Physiol 281:H1346–H1352
20. Kitagawa Y, Yamashita D, Ito H, Takaki M (2004) Reversible effects of isoproterenol-induced hypertrophy on in situ left ventricular function in rat hearts. Am J Physiol Heart Circ Physiol 28:H277–H285
21. Tachibana H, Takaki M, Lee S, Ito H, Yamaguchi H, Suga H (1997) New mechanoenergetic evaluation of left ventricular contractility in in situ rat hearts. Am J Physiol Heart Circ Physiol 272:H2671–H2678
22. Takaki M (2004) Left ventricular mechanoenergetics in small animals. Jpn J Physiol 54:175–207
23. Takeshita D, Shimizu J, Kitagawa Y, Yamashita D, Tohne K, Nakajima-Takenaka C, Ito H, Takaki M (2008) Isoproterenol-induced hypertrophied rat hearts: does short-term treatment correspond to long-term treatment? J Physiol Sci 58:179–188
24. Kuzumoto N, Kitagawa Y, Uemura K, Ueyama T, Yoshida K, Furuya H, Takaki M (2004) A brief regional ischemic-reperfusion enhances propofol-induced depression in left ventricular function of in situ rat hearts. Anesthesiology 101:879–887
25. Nakahashi K, Kitagawa Y, Ito H, Kuzumoto N, Furuya H, Takaki M (2005) Positive inotropic effect of nicorandil in in situ adult rats. J Anesth 19:45–53
26. French JP, Quindry JC, Falk DJ, Staib JL, Lee Y, Wang KKW, Powers SK (2006) Ischemia–reperfusion-induced calpain activation and SERCA2a degradation are attenuated by exercise training and calpain inhibition. Am J Physiol Heart Circ Physiol 290:H128–H136
27. Yoshikawa Y, Zhang G-X, Obata K, Matsuyoshi H, Asada K, Taniguchi S, Takaki M (2010) A cardioprotective agent of a novel calpain inhibitor, SNJ-1945 exerts β_1-actions on left ventricular mechanical work and energetics. Am J Physiol Heart Circ Physiol 299:H396–H401
28. Towbin H, Staehelin T, Gordon J (1979) Electrophoretic transfer of proteins from polyacrylamide gels to nitrocellulose sheets: procedure and some applications. Proc Natl Acad Sci USA 76:4350–4354
29. Yoshida K, Yamasaki Y, Kawashima S (1993) Calpain activity alters rat myocardial subfractions after ischemia and reperfusion. Biochim Biophys Acta 1182:215–220
30. French JP, Hamilton KL, Quindry JC, Lee Y, Upchurch PA, Powers SK (2008) Exercise-induced protection against myocardial apoptosis and necrosis: MnSOD, calcium-handling proteins, and calpain. FASEB J 22:2862–2871
31. Nakamura M, Sunagawa M, Kosugi T, Sperelakis N (2000) Actin filament disruption inhibits L-type Ca^{2+} channel current in cultured vascular smooth muscle cells. Am J Physiol Cell Physiol 279:C480–C487